Small-scale Fading Evaluation in Vehicular-to-Vehicular Communications

[1]Juan Reig, [1]Lorenzo Rubio, [2]Mengru Wang, [3]Herman Fernández, and [1]Vicent M. Rodrigo-Peñarrocha

[1] Electromagnetic Radiation Group (GRE), Instituto Universitario de Telecomunicaciones y Aplicaciones Multimedia (iTEAM), Universitat Politècnica de València, 8G Building - access D - Camino de Vera s/n, 46022 Valencia, Spain.

[2]School of Information & Communication Engineering, Beijing University of Posts and Telecommunications (BUPT), P.O.Box 151, No.10 Xitucheng Rd., Haidian Dist. Beijing, 100876, China.

[3]Escuela de Ingeniería Electrónica, Universidad Pedagógica y Tecnológica de Colombia, Sogamoso, Colombia.

Corresponding author: jreigp@dcom.upv.es

Abstract

Vehicular-to-Vehicular (V2V) communications are receiving considerable attention due to the introduction of the intelligent transport system (ITS) concept. To design, evaluate and optimize ITS applications oriented to vehicular safety based on wireless systems, the knowledge of the propagation channel is vital, in particular the small-scale fading distribution. From a narrow-band V2V channel measurements campaign carried out in an expressway area near the city of Valencia (Spain), this paper analyzes the experimental distribution of the small-scale fading. This experimental distribution is compared to the analytical distributions used in wireless communications to model the fast fading: the Rayleigh, Nakagami-*m*, Weibull, Rice and α-μ distributions.

Keywords: Vehicular communications, V2V channels, small-scale fading.

1. Introduction

Traffic accidents are an important health and social problem all over the world. In spite of the continuous reduction of the number of fatalities and injured people in traffic accidents over the last decade in developed countries, crash rates remain approximately constant in such countries [1]. This decrease in death and injured people has been achieved by both law enforcement and passive vehicle safety systems (e.g., airbags, anti-lock braking system and electronic stability control). A relevant aspect of the Intelligent Transportation Systems (ITS), which consists of the application of advanced and emerging technologies in transportation to save lives, time, money, energy and the environment, is the vehicular communications systems. A myriad of applications related to vehicles, vehicle traffic, drivers, passengers and pedestrians, which have been proposed recently, requires reliable low-latency wireless communications in vehicular ad hoc networks (VANETs). The interchange of information in such networks is achieved by vehicle-to-vehicle (V2V) and vehicle-to-infrastructure (V2I) communications. VANET also enables to extend the range of the communications by using the multiple-hop mode. Thus, several services as hazard warnings or information on the current traffic situation will be addressed with minimal latency in these wireless cooperative systems. Physically, radio transmitter on-board units (OBUs) inside the vehicles, and access points placed along the road, equipped with radio transmitter road-side units (RSUs), make vehicular communications operational.

In USA, the first ITS services, such as the electronic toll collection, were allocated in a frequency spectrum between 902 MHz and 928 MHz [2], whereas the band of 5.8 GHz (5.795-5.815 GHz) was allocated in Europe as a part of dedicated short-range communications (DSRC) bands [3]. Unfortunately, this band turned out to be insufficient for high and medium-range vehicular communication systems. Therefore, the Federal Communication Commission (FCC) assigned 75 MHz of licensed spectrum in the 5.9 GHz frequency band in 1999, concretely from 5.850 GHz to 5.925 GHz [4], see Fig. 1. Its importance is further highlighted by the European decision on the use of the 5.875-5.905 GHz frequency band for safety-related ITS applications and later on, the 5.855-5.875 GHz and 5.905-5.925 GHz bands for non-safety-related and road safety and traffic efficiency services, respectively [5], [6].

In USA, the FCC specified the list of channels using 10 or 20 MHz bandwidth for DSRC applications, even though

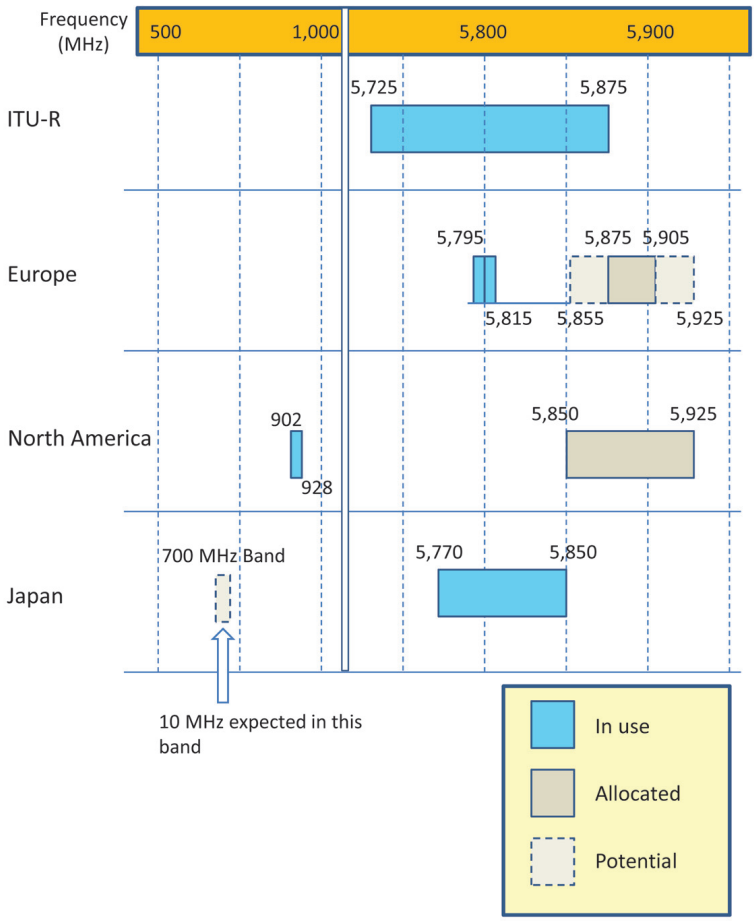

Figure 1. Spectrum allocated for ITS systems [22].

10 MHz is the most common channelization proposed for ITS. For instance, channel 178 is the control channel (CCH) used to broadcast communications related to safety applications. Service channels (SCHs) are dedicated to safety and non-safety applications. Channels 172 and 184 are especially used to V2V and V2I communications for safety applications in crossroad situation, respectively. The maximum equivalent isotropically radiated power (EIRP) for DSRC devices, i.e., OBUs and RSUs, is also illustrated in Fig. 2, where we have distinguished between public (Pub.) and private (Priv.) applications [4].

In 2006, the family of standards named as Wireless Access in Vehicular Environments (WAVE) [7] was issued by the IEEE to promote ubiquitous high-speed communications between vehicles and service providers, and homogeneous communications interfaces between different automotive manufacturers.

Fig. 3 illustrates the WAVE protocol stack for DSRC communications, including acronyms of protocols and standards [8]. At the physical (PHY) and medium access control (MAC) layers, DSRC makes use of the IEEE 802.11p

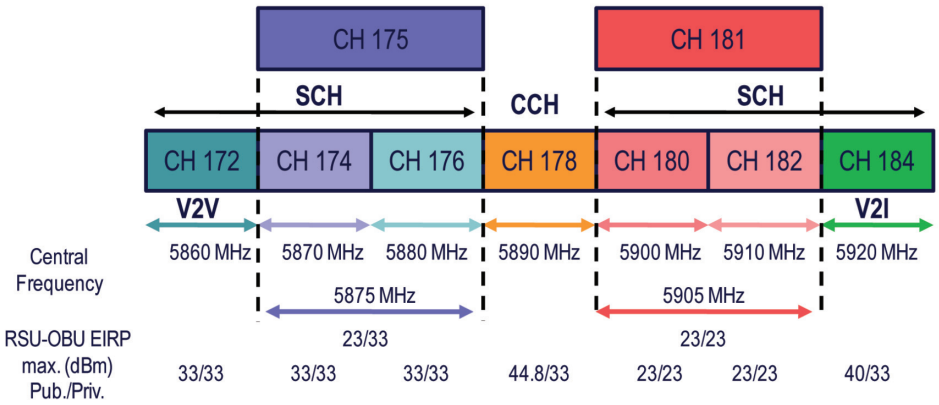

Figure 2. DSRC channel allocation in the 5.9 GHz band for ITS applications in USA [23]

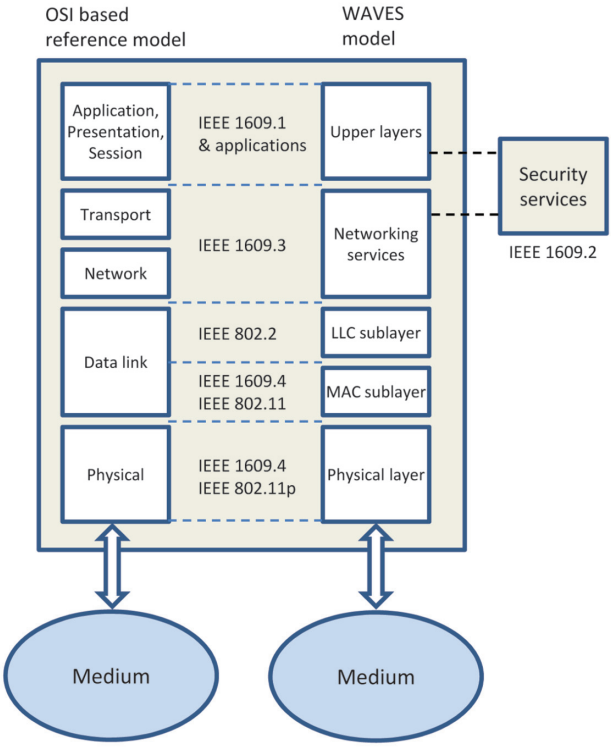

Figure 3. WAVE protocol suites, based on [8].

specifications [9], a modified version of the IEEE 802.11 (WiFi) OFDM standard [10], defined previously by the American Society for Testing and Materials (ASTM) in 2003. In the middle of the stack, DSRC employs a suite of standards defined by the IEEE 1609 Working Group: 1609.4 for Channel Switching, 1609.3 for Network Services (including the WAVE Short Message Protocol VWSMP), and 1609.2 for Security Services. DSRC also supports the use of the well-known Internet protocols for the Network and Transport layers, i.e., Internet Protocol version 6 (IPv6), user datagram protocol (UDP) and transmission control protocol (TCP). IEEE 802.11p is also one mode of communication access for land mobiles (CALM), a framework for heterogeneous packet-switched communications in mobile environments approved by the International Standards Organization (ISO).

In the PHY layer, the basic parameters of the IEEE 802.11p, which correspond to the 802.11 OFDM are illustrated in Table 1 for a 10 MHz channelization [10]. The number of data subcarriers is N_{SD} = 48. Four modulation schemes can be used by subcarrier, each of which corresponds to a different number of bits encoded per subcarrier symbol, N_{DBPS} (see Table 2). Convolutional codes of different coding rates, r, are available. Eight combinations of modulation scheme and coding rate are specified in IEEE 802.11 [10].

Channel models for traditional fixed-to-mobile communications cannot be applied to assess the performance of ITS applications based on vehicular communications systems.

The data rate can be calculated as

$$R = \frac{N_{DBPS}}{T_{SYM}} = \frac{N_{SD} r \log_2 M}{T_{SYM}}, \quad (1)$$

where T_{SYM} is the symbol period and M is the number of points of the constellation in the modulation scheme.

For instance, the data rate of the channel for the QPSK modulation (M = 4) and rate r = 1/2 of the convolutional code, is given by

$$R = \frac{48 \times \frac{1}{2} \times \log_2 4 \text{ bit}}{8 \cdot 10^{-6} \text{ s}} = 6 \text{ Mb/s}. \quad (2)$$

Note that the control channel 178 in USA uses the above combination of modulation and rate.

Due to the characteristic of low latency in communications oriented to vehicular safety, a precise understanding of the propagation channel is essential to design, evaluate and optimize the future vehicular communication applications. The vehicular propagation channel, where both the transmitter (Tx) and the receiver (Rx) can be in motion with low elevation antennas, exhibits significant differences compared to the traditional fixed-to-mobile (F2M) channels. Such discrepancies produce that channel models for F2M communications cannot be applied to assess the performance of ITS applications based on vehicular communications systems. In addition, the propa-

Parameter	Value
Channel spacing	10 MHz
Occupied bandwidth	8.3 MHz
Number of data subcarriers, N_{SD}	48
Number of pilot subcarriers, N_{SP}	4
Subcarrier frequency spacing, Δ_F	156.25 kHz = 10 MHz/64
Fast Fourier period, T_{FFT}	6.4 μs = 1/ T_{FFT}
Guard interval duration, T_{GI}	1.6 μs = T_{FFT} /4
Symbol period, T_{SYM}	8 μs = T_{GI} +T_{FFT}
Error correction code	Convolutional code K=7 (64 states)

Table 1. Basic parameters of IEEE 802.11 OFDM with 10 MHz spacing [10].

Modulation	Coding rate R	Coded bits per OFDM symbol N_{CBPS}	Data bits per OFDM symbol N_{DBPS}	Data rate Mb/s
BPSK	1/2	48	24	3
BPSK	3/4	48	36	4.5
QPSK	1/2	96	48	6
QPSK	3/4	96	72	9
16-QAM	1/2	192	96	12
16-QAM	3/4	192	144	18
64-QAM	2/3	288	192	24
64-QAM	3/4	288	216	27

Table 2. Modulation parameters of IEEE 802.11 OFDM with 10 MHz spacing [10].

gation mechanisms in the DSRC band are significantly different to those are present in the traditional cellular communications bands, i.e., from 1 to 2 GHz.

Over the past ten years, the vehicular channel has attracted the interest of numerous researchers [11]-[15]. Nevertheless, a specific fading analysis has not been performed in V2V communications. Based on an extensive measurement campaign, researchers of the Electromagnetic Radiation Group (ERG) at the iTEAM Research Institute have assessed the characteristics of the small-scale and long-term fading in V2V links. This work analyzes thoroughly the small-scale behavior of the V2V channel in an expressway scenario due to the multipath propagation, as it is shown in Fig. 4.

This paper is organized as follows. In Section 2, the measurement campaign and setup are introduced. Section 3 describes an extensive analysis of the statistical distributions used to model the small-scale fading. Also results of both Kolmogorov-Smirnov (K-S) fulfillment test and estimated parameters for small-scale distributions are analyzed in this Section. Finally, the conclusions are discussed in Section 4.

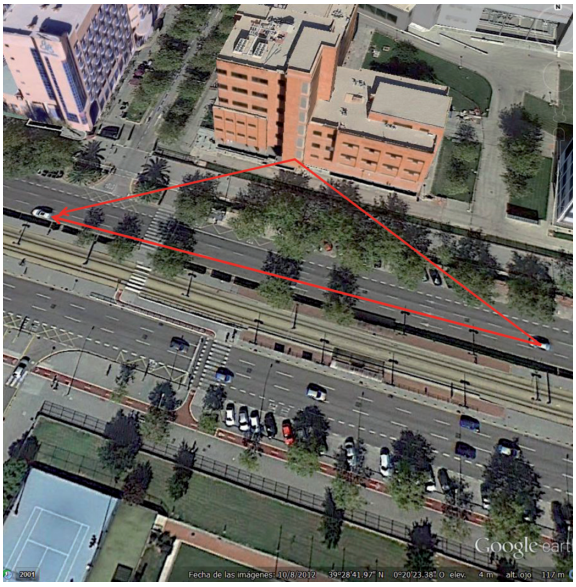

Figure 4. Example of the vehicular to vehicular communications link.

2. Channel measurements

In V2V communications, the considerable mobility of both the Tx and Rx terminals and the interacting objects (reflectors and/or scatterers), leads to high temporal variability (time-selectivity). In addition, the low elevation antennas along with the displacement of the interacting objects, and a significant probability of Tx-Rx link obstruction, determine the range of the communications, particularly in heavy traffic urban environments. Therefore, accurate models for the fading distribution are essential to develop, evaluate and validate new protocols and system architecture configurations. Vehicular networks simulators require the integration of realistic propagation channels, to which may also be added mobility models to take into account the behavior of vehicles. It is worth highlighting that in the context of vehicular networks, simulations are particularly decisive due to the difficulty and enormous effort to perform real tests involving the high number of vehicles, driving conditions and different vehicular environments.

2.1. Measurement setup

In order to characterize the V2V channel, a channel sounder has been designed at the above mentioned DSRC frequency of 5.9 GHz. This system was designed for the measurement in a narrow-band vehicular communications channel to estimate the path loss, Doppler effect and fading statistics.

On one hand, as it is shown in Fig. 5, the HP83623A Signal Generator (SG) was used to obtain a 5.9 GHz Continuous Wave (CW) at the Tx. A power amplifier enables to transmit with 23.8 dBm of EIRP. On the other hand, the ZVA24 Rohde & Schwarz Vector Network Analyzer (VNA) was in charge of estimating the received power level, measuring, directly, the b_2 parameter, at the Rx. A laptop controlled the VNA to automate the measurements acquisition system. Furthermore, we used two amplifiers in series and low loss wires with 1.15 dB at 5.9 GHz, to achieve a total gain of 68.12 dB. The received system is shown in Fig. 6.

The noise level and the bandwidth resolution have been

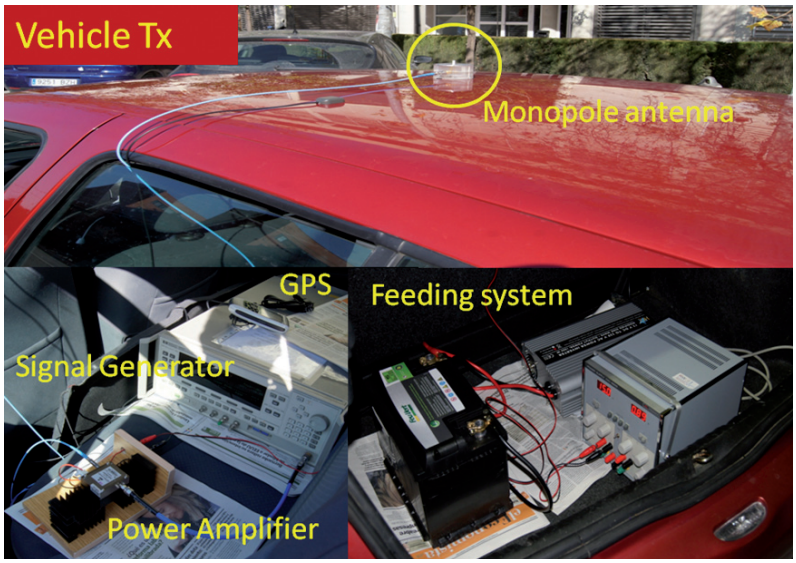

Figure 5. Transmitter system setup for the channel sounder.

Figure 6. Receiver system setup for the channel sounder.

measured in the laboratory. The results show that using a resolution bandwidth (RBW) of 10 kHz leads to both a noise level of -80 dBm and an acquisition measurement time of 135 μs. However, the noise level reaches -75 dBm and 45 μs of acquisition time with a RBW of 100 kHz.

Both Tx and Rx use the same antenna, a $\lambda/4$ monopole, which provides a gain in the horizontal plane of -2.56 dB measured in an anechoic chamber with the scattering parameter S_{11} lower than -21 dB at 5.9 GHz.

In addition, both the Tx and Rx systems were equipped with a GPS receiver, each one controlled by a laptop, to provide constant information about the acquisition measurement time, as well as relative speed and separation distance between Tx and Rx. The laptops have been synchronized to relate the data from the different GPS and the measurement from the VNA.

A power supply system is required for the measurement system equipment aboard vehicles. A couple of 75 Ah, 12 V DC battery along with an inverter to convert to 220 V AC supply around 90 minutes of autonomy, enough time to perform the measurement campaign.

2.2. Measurement environment

This environment corresponds to an expressway in the north of the city of Valencia, with heavy road traffic density and three lanes in each direction. Both sides of the expressway are open areas. The total path is depicted in Fig. 7. Details about the measurements are shown in Table 3.

In order to analyze the small-scale statistics, the total measurement record has been divided in windows of 100λ, which correspond to a variable window size in number of samples because of the variation of the receiver vehicle speed. Table 4 shows the main parameters of each window. The low mean standard deviation of the received power reflects a dominant multipath component in most of the extracted windows.

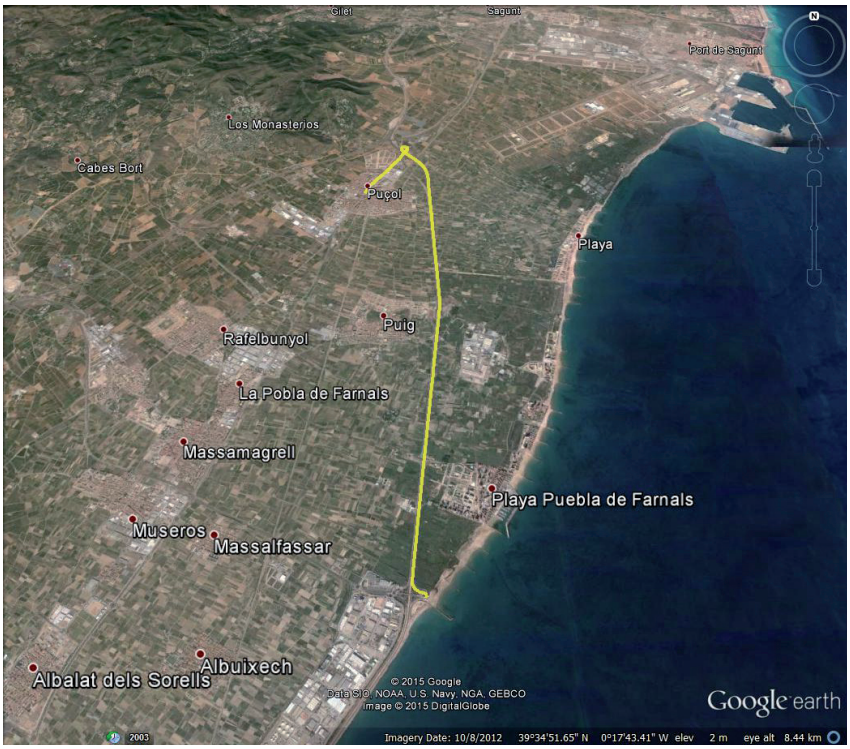

Figure 7. Path driven in the measurement campaign.

Number of samples	Total duration	Total distance	Mean time between samples	Mean distance covered between samples
595,000	602.78 s	10,762.76 m	1.013 ms	0.018 m

Table 3. Main parameters of the V2V measurements.

Number of windows	Mean size in samples	Mean relative speed	Max. relative speed	Mean distance between Tx and Rx	Max. distance between Tx and Rx	Mean standard deviation of the received power
2112	281.72	16.31 km/h	49.14 km/h	163.3 m	440.53 m	2.16 dB

Table 4. Parameters using short-term windows of 100λ.

3. Estimators of the small-scale distributions

In this section, some estimators of the Rayleigh, Rice, Weibull, Nakagami-m, α-μ distributions are used to model the small-scale fading in vehicular communications. Such distributions have been extensively used in F2M environments [16]. Nevertheless, some researchers have employed them to characterize the small-scale fading in the vehicular communications channel [17], [18].

First of all, we analyze the standard deviation of the field strength in logarithmic units using a fixed-size window. Second, we present the percentage of fulfillment of the K-S test for the small-scale distributions in all the records. Finally, the distributions of the estimated parameters for such distributions are analyzed thoroughly.

3.1. Standard deviation of the field strength

The standard deviation of the field strength in dBV/m has been calculated for all the windows with a size of 100λ. Fig. 8 shows the standard deviation of the field strength in terms of the separation between the Tx and Rx vehicles. Each dot represents the standard deviation in dB in a window of size 100λ. It can be observed a high dispersion of the standard deviation with high concentration between 0.5 and 3 dB, which are small values of standard deviations for the small-scale fading in F2M communications. Nevertheless, 2.5% of 100λ-sized windows provide standard deviations that exceed 5.57 dB. Note that this situation corresponds to a composite small-scale and long-term fading. Meanwhile, the standard deviation of the field strength is also shown in Fig. 9 in terms of the absolute relative speed between the Tx and Rx, v_{rel}.

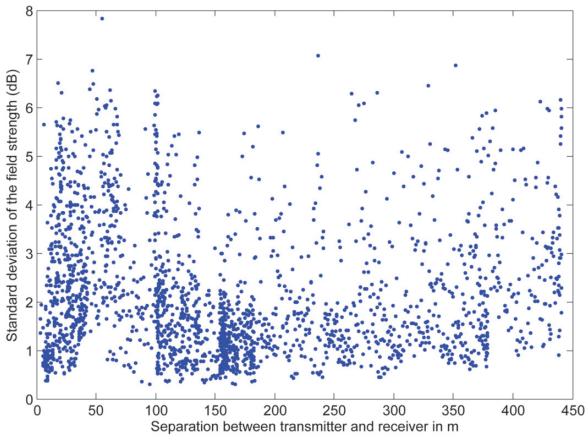

Figure 8. Standard deviation in dB of the field strength in dBV/m as a function of the separation between transmitter and receiver in m.

This absolute relative speed is defined as

$$v_{\text{rel}} = \left| v_{\text{Tx}} - v_{\text{Rx}} \right|, \tag{3}$$

where $|\cdot|$ represents the absolute value, and v_{Tx} and v_{Rx} are the Tx and Rx speeds, respectively.

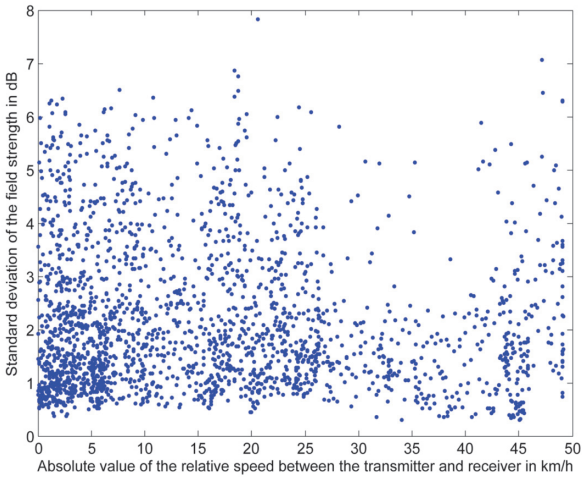

Figure 9. Standard deviation in dB of the field strength in dBV/m as a function of the absolute value of the relative speed between the transmitter and receiver in km/h.

From Fig. 9, it can be inferred that the standard deviations barely depend on the absolute value of the relative speed in V2V communications.

3.2. Kolmogorov-Smirnov test

Once calculated the estimated parameters of the Rayleigh, Rice, Nakagami-m, Weibull, and α-μ distributions, we have compared such distributions to the experimental distribution in each window. The statistical K-S test is used to assess the goodness-of-fit of the above estimated distributions to the experimental results [19].

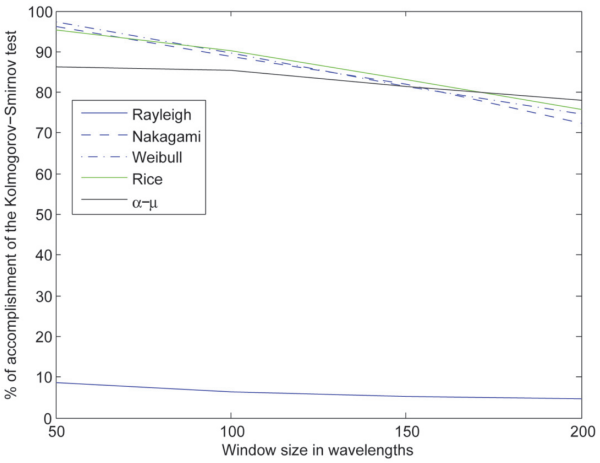

Figure 10. Percentage of accomplishment of the Kolmogorov-Smirnov test for a significance of 1% as a function of the window size in wavelengths.

To determine the optimal size of the windows, we have calculated the percentage of fulfillment of the K-S test for the above distribution as a function of the window sizes in wavelengths for a significance of 1%, as depicted in Fig. 10.

From Fig. 10, the percentage of accomplishment decreases with the window size for all the analyzed distributions. However, this percentage tends to stabilize for window sizes lower than 100λ for the α-μ distribution. Therefore, we have evaluated the K-S test using a window size of 100λ to maximize the number of samples in each extracted window.

An example of evaluation of the K-S test applied to the Rayleigh distribution is shown in Fig. 11 by using the cumulative distribution function (CDF). The K-S test in one extracted window given is fulfilled if the maximum absolute value between the experimental and the estimated distribution, $D_{\text{estimated}}$, depicted with double arrows lines in Fig. 11, is lower or equal than a given value, $K_n(p)$,

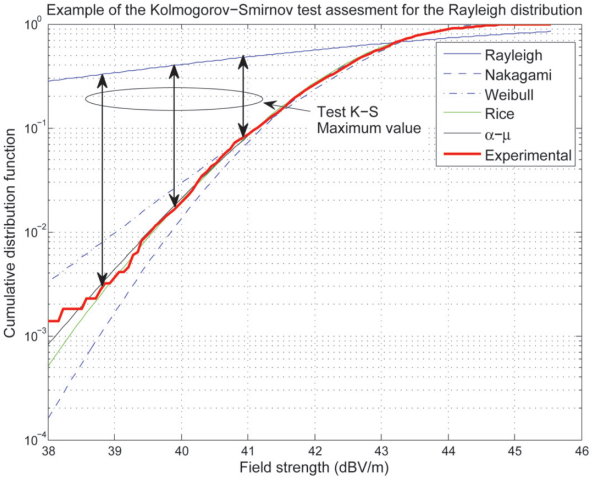

Figure 11. Example of the evaluation of the Kolmogorov-Smirnov test using the cumulative distribution function for the Rayleigh distribution.

which depends on both the number of samples, n, and the significance level, p. Therefore, the condition to be fulfilled in each window is as follows

$$D_{\text{estimated}} = \max_{i=1,\ldots,N} \left| \hat{F}_{\text{estimated}}(x_i) - F_{\text{experimental}}(x_i) \right| \leq k_n(p), \quad (4)$$

where $\hat{F}_{\text{estimated}}(\cdot)$ is the CDF of the Rayleigh, Nakagami-m, Weibull, Rice or α-μ estimated distributions, $F_{\text{experimental}}(\cdot)$ is the CDF of the experimental distribution, and

$$k_n(p) = \begin{cases} \dfrac{1.63}{\sqrt{n}}, & p = 1\% \quad n > 50 \\ \dfrac{1.36}{\sqrt{n}}, & p = 5\% \quad n > 50 \end{cases} \quad (5)$$

The statistical K-S test has been assessed for the Rayleigh, Nakagami-m, Weibull, Rice, and α-μ distributions in the 2,112 windows with sizes of 100λ. Table 5 shows the percentage of fulfillment of K-S test with significance levels of 5% and 1%. Also, the percentage of the best-fit distribution is illustrated in Table 5. This percentage evaluates the number of the windows for each estimated distribution where the value of $D_{\text{estimated}}$ is the least amongst the values of the rest of the estimated distributions, divided by the total of windows, i.e., 2,112. Note that the sum of the percentages of the best-fit distribution for all distributions is equal to 100%.

From Table 5, the Nakagami-m, Weibull, Rice, and α-μ distributions match rather satisfactorily the experimental distribution with similar percentages of accomplishment over 78%. Nevertheless, the α-μ distribution clearly is the best-fit distribution, condition fulfilled in the 46.31% of the cases.

3.3. Distribution of estimated parameters.

Once the parameters of the Rayleigh, Nakagami-m, Weibull, Rice, and α-μ distributions are estimated, we can obtain the distribution of the main parameters of these statistics for all the measurements.

Since all the distributions of these parameters are considerably right-skewed, we have obtained the distribution for each parameter in logarithm units, i.e., 10 log p, where p is the parameter analyzed.

The skewness is a measure of the asymmetry of the probability distribution [20]. It is defined as

$$\hat{\gamma}_1 = \frac{\hat{\mu}_3}{\hat{\mu}_2^{3/2}}, \quad (6)$$

where $\hat{\mu}_n$ is the nth sample central moment of the distribution. If $\hat{\gamma}_1 = 0$ the distribution is symmetrical. Values of right-skewed distributions provide $\hat{\gamma}_1 > 0$, and $\gamma_1 < 0$ corresponds to left-skewed distributions.

The kurtosis is a measure of the "peakedness" of the probability distribution [20]. It is defined as

$$\hat{\beta}_2 = \frac{\hat{\mu}_4}{\hat{\mu}_2^2}. \quad (7)$$

For instance, a Gaussian distribution exhibits $\hat{\gamma}_1 = 0$ and $\hat{\beta}_2 = 3$.

Table 6 shows the sample mean, standard deviation, skewness, and kurtosis of the main parameters of the estimated distributions in logarithmic units. For further details about the definition of the parameters and the estimators of such distribution, the reader is referred to [21].

Distribution		Rayleigh	Nakagami-m	Weibull	Rice	α-μ
K-S	5%	4.5	80.82	78.27	81.77	82.01
	1%	6.4	88.87	89.73	90.24	85.46
	Best-fit %	0.66	14.63	24.72	13.68	46.31

Table 5. Best-fit distributions percentages and fulfillment percentage of the Kolmogorov-Smirnov test for a significance level of 5% and 1%, with window sizes of 100 wavelengths.

Distribution Parameter	Nakagami m	Weibull α	Rice K	α-μ α	α-μ μ
Mean (dB)	8.54	7.96	10.91	5.48	4.92
Std. dev (dB)	5.39	2.75	5.57	5.52	9.08
Kurtosis	2.58	2.36	2.84	5.99	6.66
Skewness	0.37	0.03	–0.17	0.65	0.91

Table 6. Sample mean, standard deviation, skewness, and kurtosis of the main parameters of the estimated distributions in logarithmic units (10 log p, where p is the parameter).

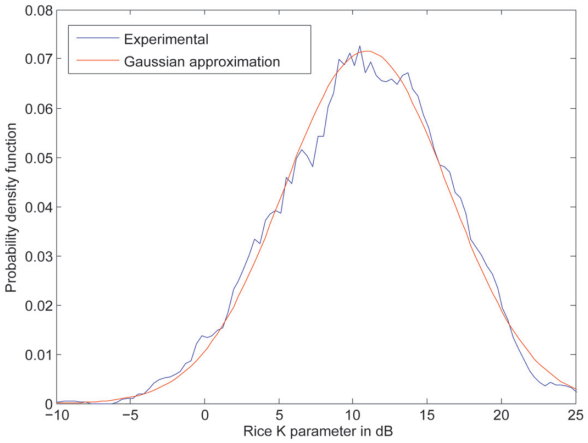

Figure 12. Probability density functions of the *K* parameter of the Rice distribution in dB and the Gaussian approximation.

All the parameters exhibit high standard deviation in dB except the α parameter of the Weibull distribution, which has a lower standard deviation of 2.75 dB.

Also, all the distributions are significantly symmetrical with maximum absolute value of the skewness of 0.91 for the μ parameter of the α-μ distribution.

Since the kurtosis and the skewness for the K(dB) of the Rice distribution are close to 3 and 0, respectively, we can approximate this distribution for a Gaussian distribution. Fig. 12 shows the probability density function of the K(dB) of the Rice distribution and the Gaussian approximation. The mean of K(dB) of 10.91 dB is considerably high and suggests a dominant multipath component prevailing in multiple windows. In the V2V communication channel at 5.9 GHz, the secondary scattered and/or reflected components are significantly attenuated related to the main contribution, and thus it results in high K(dB) parameter values.

4. Conclusions

In this work, an extensive study of the small-scale amplitude distribution in the V2V channel has been carried out in the 5.9 GHz band in an expressway environment.

Parameters of the Rayleigh, Rice, Nakagami-m, Weibull, and α-μ distributions have been estimated and such inferred distributions are compared to the experimental distribution using the K-S test for all the windows. With the help of the K-S test, we have shown that the α-μ distribution is the most frequently best-fit distribution. To extract the small-scale fading, we have divided the total record in windows of sizes 100λ.

Finally, we have observed that the Rice *K* parameter can be modeled as a lognormal distribution with a considerable mean, 10.91 dB, which corresponds to a dominant component in multiple windows.

Acknowledgments

The authors want to thank J. A. Campuzano, D. Balaguer and L. Moragón for their support during the measurement campaign, as well as B. Bernardo-Clemente and A. Vila-Jiménez for their support and assistance in the laboratory activities. This work has been funded in part by the Programa Estatal de Fomento de la Investigación Científica y Técnica de Excelencia. Ministerio de Economía y Competitividad, Spain, TEC2013-47360-C3-3-P.

References

[1] World Health Organization. Global Status Report on Road Safety 2013. http://www.who.int/violence_injury_prevention/road_safety_status/2013/en/

[2] ASTM E2158-01, Standard Specification for Dedicated Short Range Communication (DSRC) Physical Layer Using Microwave in the 902 to 928 MHz Band (Withdrawn 2010), ASTM International, West Conshohocken, PA, USA, 2001.

[3] CEN TC 278 EN 12253 Dedicated Short-Range Communication – Physical layer using microwave at 5.8 GHz. European Committee for Standardization (CEN), Central Secretariat, Brussels, Belgium, 2004.

[4] ASTM E2213–03. Standard Specification for Telecommunications and Information Exchange Between Roadside and Vehicle Systems — 5 GHz Band Dedicated Short Range Communications (DSRC) Medium Access Control (MAC) and Physical Layer (PHY) Specifications, American Society for Testing Materials (ASTM), West Conshohocken, PA, USA. 2003.

[5] ETSI TR 102 492-1 V1.1.1 (2005-06), Technical Report; Electromagnetic Compatibility and Radio Spectrum Matters (ERM); Intelligent Transport Systems (ITS); Part 1: Technical Characteristics for Pan-European Harmonized Communications Equipment Operating in the 5 GHz Frequency Range and Intended for Critical Road-Safety Applications; System Reference Document. European Telecommunications Standards Institute, Sofia, Antipolis, France, 2005.

[6] ETSI TR 102 492-2 V1.1.1 (2006-07), Electromagnetic Compatibility and Radio Spectrum Matters (ERM); Intelligent Transport Systems (ITS); Part 2: Technical Characteristics for Pan European Harmonized Communications Equipment Operating in the 5 GHz Frequency Range Intended for Road Safety and Traffic Management, and for Non-safety Related its Applications; System Reference Document. European Telecommunications Standards Institute, Sofia, Antipolis, France, 2006.

[7] IEEE 1609 - Family of Standards for Wireless Access in Vehicular Environments (WAVE). http://www.standards.its.dot.gov D. Khijniak, WAVE Prototype and Algorithms based on the IEEE 802.11p Standard, in GLOBECOM 2008 Design and Developers Forum. IEEE Communications Society, December 2008, slides presented during the Design and Developers Forum: DD03M2, IEEE GLOBECOM 2008.

[8] D. Khijniak, WAVE Prototype and Algorithms based on the IEEE 802.11p Standard, in GLOBECOM 2008 Design and Developers Forum. IEEE Communications Society, December 2008, slides presented during the Design and Developers Forum: DD03M2, IEEE GLOBECOM 2008.

[9] IEEE 802.11. IEEE Standard for Information Technology-Telecommunications and Information Exchange between Systems Local and Metropolitan Area Networks-Specific Requirements. Part 11: Wireless LAN Medium Access Control (MAC) and Physical Layer (PHY) Specifications. Amendment 6. Wireless Access in Vehicular Environments. The Institute of Electrical and Electronic Engineers, NY, USA, 2010.

[10] IEEE 802.11. IEEE Standard for Information Technology-Telecommunications and Information Exchange between Systems Local and Metropolitan Area Networks-Specific Requirements. Part 11: Wireless LAN Medium Access Control (MAC) and Physical Layer (PHY) Specifications. The Institute of Electrical and Electronic Engineers, NY, USA, 2012.

[11] I. Sen and D. W. Matolak. Vehicle–Vehicle Channel Models for the 5-GHz Band, IEEE Transactions on Intelligent Transportation Systems, vol.9, no.2, pp. 235-245, Jun. 2008.

[12] A. F. Molisch, F. Tufvesson, J. Karedal, and C. F. Mecklenbrauker. A Survey on Vehicle-to-Vehicle Propagation Channels, IEEE Wireless Communications, vol.16, no.6, pp.12,22, Dec. 2009.

[13] L. Rubio, J. Reig and H. Hernandez. Propagation Aspects in Vehicular Networks. Vehicular Technologies: Increasing Connectivity. Miguel Almeida (Ed.): InTech, 2011. Available at: http://www.intechopen.com/books/vehicular-technologies-increasing-connectivity/propagation-aspects-in-vehicular-networks.

[14] H. Fernández, L. Rubio, J. Reig, V. M. Rodrigo-Peñarrocha, and A. Valero. Path Loss Modeling for Vehicular System Performance and Communication Protocols Evaluation, Mobile Network Applications, Springer, vol. 18, pp. 755–765, 2013.

[15] H. Fernandez, L. Rubio, V. M. Rodrigo-Peñarrocha, and J. Reig, Path Loss Characterization for Vehicular Communications at 700 MHz and 5.9 GHz Under LOS and NLOS Conditions. IEEE Antennas and Wireless Propagation Letters, vol.13, pp. 931-934, 2014.

[16] Y. Karasawa and H. Iwai. Modeling of Signal Envelope Correlation of Line-of-sight Fading with Applications to Frequency Correlation Analysis. IEEE Transactions on Communications, vol. 42, no.6, pp. 2201-2203, Jun. 1994.

[17] Lin Cheng, B. E. Henty, D. D. Stancil, Fan Bai, and P. Mudalige, Mobile Vehicle-to-Vehicle Narrow-Band Channel Measurement and Characterization of the 5.9 GHz Dedicated Short Range Communication (DSRC) Frequency Band. IEEE Journal on Selected Areas in Communications, vol.25, no.8, pp.1501-1516, Oct. 2007.

[18] O. Renaudin, V-M. Kolmonen, P. Vainikainen, and C. Oestges. Car-to-car Channel Models Based on Wideband MIMO Measurements at 5.3 GHz. European Conference on Antennas and Propagation, pp. 635-639, Berlin, Germany, Mar. 2009.

[19] A. N. Kolmogorov. Selected works, vol. II: Probability Theory and Mathematical Statistics (with a Preface by Aleksandrov, P.S.; Translated from the Russian by Lindquist, G.; Translation Edited by Shiryayev, A.N.). Kluwer Academic Publishers Group, Dordrecht, 1992.

[20] N. L. Johnson, S. Kotz, and N. Balakrishnan. Continuous Univariate Distributions, Vol 1, 2nd Edition, Wiley, 1994.

[21] J. Reig, M.-T. Martínez-Inglés, L. Rubio, V.-M. Rodrigo-Peñarrocha, and J.-M. Molina-García-Pardo. Fading Evaluation in the 60 GHz Band in Line-of-Sight Conditions, International Journal of Antennas and Propagation, Hindawi, vol. 2014, 2014.

[22] S. Oyama. Activities on ITS Radio communications Standards in ITUR and in Japan, in 1st ETSI TC-ITS Workshop. ETSI, February 2009, slides presented during the 1st ETSI TC-ITS Workshop 2009, Sophia Antipolis, France.

[23] A. J. Campuzano, H. Fernández, D. Balaguer, A. Vila, B. Bernardo-Clemente, V. M. Rodrigo-Peñarrocha, J. Reig, A. Valero-Nogueira, and L. Rubio. Vehicular-to-Vehicular Channel Characterization and Measurement Results. WAVES, Universitat Politècnica de València, 2012.

Biographies

Juan Reig was born in Alcoy, Spain, in 1969. He received the M.S. and Ph.D. degrees in Telecommunications Engineering from the Universitat Politècnica de Valencia (UPV), Spain, in 1993 and 2000, respectively. He has been a faculty member in the Department of Communications at the Technical University of Valencia, Spain since 1994, where he is now Associate Professor of Telecommunication Engineering. He is a member of the Radio and Wireless Communications Group (RWCG) of the Telecommunications and Multimedia Applications Research Institute (iTEAM). His areas of interest include fading theory, diversity, ultra-wide band systems and vehicular communications in V2V and V2I networks.

Lorenzo Rubio was born in El Ballestero, Albacete, Spain, in 1971. He received the M.S. and the Ph.D degrees in Telecommunications Engineering from the Universitat Politècnica de València, Spain, in 1996 and 2004, respectively. In 1996, he joined the Communications Department of the Universitat Politècnica de València (UPV), where he is now Associate Professor of wireless communications. His main research interests are related to wireless communications. Specific current research topics include radiowave propagation, measurement and mobile time-varying channels modelling in vehicular applications, ultra-wideband (UWB) communication systems, multiple-input multiple-output (MIMO) systems and equalization techniques in digital wireless systems. Dr. Rubio was awarded by the Ericsson Mobile Communications Prize from the Spanish Telecommunications Engineer Association for his study on urban statistical radiochannels characterization applied to wireless communications.

Mengru Wang was born in TianJin, China in 1993. She is a Telecommunication Engineering student at the Beijing University of Posts and Telecommunications (BUPT). Meanwhile, she has the double degree at Queen Mary university of London. Currently, she is as an interchange student to finish the final project in Universitat Politècnica de València (UPV). Her current research interests include radiowave propagation and vehicular communications.

Herman Fernández was born in Bogota, Colombia in 1972. He received the Electronic Engineering degree from the Universidad Autónoma de Colombia, in 1997, the M.S. degree in Electrical Engineering from the Universidad de los Andes, Colombia, in 1999, the M.S. degree in Engineering-Industrial Automation from the Universidad Nacional, Colombia, in 2007, and M.S. and Ph.D. degrees in Systems and Communications Networks and in Telecommunication from the Universitat Politècnica de València, Spain, in 2011 and 2014, respectively. He has been a faculty member in the Department of Electronic at the Universidad Pedagógica y Tecnológica de Colombia, where he is now Associate Professor of Electronic Engineering. His research interests include wireless communications and propagation modeling. His current research is focused on channel measurements and modeling in vehicular-to-vehicular (V2V) communications.

Vicent Miquel Rodrigo Peñarrocha was born in Valencia, Spain, on 1966. He received the Ingeniero de Telecomunicación degree in 1990 from the Universidad Politécnica de Madrid (UPM) and the PhD in 2003 from the Universidad Politécnica de Valencia (UPV). He joined the Departamento de Comunicaciones at the UPV in 1991 as a Lecturer. His current interests include radiowave propagation, antenna measurements, instrumentation, virtual instrumentation and laboratories and any educational activity problems.